

Obstacle Avoidance Path Design for Autonomous Vehicles – A Review

Ahmed Tijani

The University of Toledo College of Engineering

Email: Ahmed.tijani@rockets.utoledo.edu

Abstract. Autonomous vehicles are the new revolution in the transportation system. They are designed to improve road efficiency and driving safety. Much research has been undertaken over the years involving significant topics, such as autonomous driving stages and safety, road formation control, obstacle detection, and obstacle avoidance strategies. The implementation of an autonomous driving system relies on several stages. Therefore, a range of different planning approaches are required to ensure safety, comfort, and efficiency. The safety aspect is one of the challenges in self-driving cars as it allows autonomous cars to navigate on the roads. Obstacle detection and obstacle avoidance systems have a major impact on autonomous driving safety. Obstacle detection utilizes the Markov random field (MRF) model that combines three potentials to segment obstacles and non-obstacles in a dangerous environment. Obstacle avoidance applies an improved artificial potential field algorithm to create a collision-free path for autonomous vehicles. In this paper, several approaches and methods are discussed for autonomous vehicles obstacle detection and avoidance systems as well as vehicle formation control techniques. A large number of relevant published papers have been systematically reviewed. Obstacle detection methods and obstacle avoidance approaches for autonomous vehicles are summarized. The results illustrate the efficiency of applied models in optimizing and improving a safe navigating path for autonomous vehicles.

Keywords. Autonomous vehicle, obstacle avoidance, formation control, Markov random field, improved artificial potential field.

1. Introduction

Autonomous vehicles are getting closer to becoming a reality. Such vehicles operate without the need for human input [1]. They rely on advanced technologies, such as sensors, cameras, radar, LiDAR, and Artificial Intelligence (AI) to become fully automated [2]. According to the World Health Organization (WHO), around 1.35 million people die every year as a result of road traffic accidents [3]. The National Highway Traffic Safety Administration (NHTSA) states that in 2019 over 37,000 people died, and more than 2 million people were injured or permanently disabled, due to car accidents in the United States [4]. The leading cause of death and injuries among children and young adults is road traffic accidents. The impact of road traffic accidents costs most countries about 3% of their gross domestic product. Speeding, distracted driving, and inadequate visibility are some of the leading factors that contribute to road crashes. Speeding is directly related to crashes or injuries. Every 1% increase in average speed generates a 4% increase in the risk of a fatal accident and a 3% increase in the risk of a crash. Distractions slow reaction times, which can cause an accident. Distracted driving is one of the major causes of traffic crashes, and is considered a threat to road safety. Distracted drivers are four times more likely to be involved in a car accident [3]. Inadequate visibility is a real problem, especially on curvy roads. A driver needs 0.5s-1s to react to an emergency situation [5]. Autonomous vehicles have the potential to improve road safety by addressing these human causes of road traffic accidents. These vehicles are designed to end human error in driving. One advantage of autonomous vehicles is to provide a safe transportation option. According to the US Department of Transportation, drivers in the US spend more than 42 hours in delays and traffic congestion every year. Human error causes 94% of collisions, which themselves provide one reason for traffic congestion and car accidents. Another benefit of having autonomous vehicles is to offer a convenient way to commute. According to a recent report, autonomous vehicles may share about one-fourth of all the miles driven in the U.S. Thus, commuters in urban areas can benefit from the most convenient form of transportation [6]. This technology will possibly revolutionize the entire transportation system and the concept of operating vehicles.

Most recent studies in the autonomous vehicle field have not focused on the effect of different driving behaviors and obstacle characteristics on path planning. Also, some approaches and methods such as vehicle kinematics, dynamics of obstacle avoidance paths, and the constraints of road boundaries have not considered. Moreover, most existing risk assessment models are complex to implement in the obstacle avoidance system. To ensure the safety of autonomous navigation, convolutional Neural Network (CNN) models, for instance, are applied in most current autonomous vehicle studies. The CNN predicts the navigating path for autonomous vehicles, relying on data collected from the sensors. However, incomplete training, inaccurate information, or the failure of any sensors would cause a collision.

This review assesses different approaches to obstacle detection and obstacle avoidance path planning design for an autonomous driving system. These approaches demonstrate the improvement of obstacle detection methods in complex environments. The integration of the Markov random field (MRF) addresses road segmentation and obstacle detection. The obstacle is segmented out from the image in the framework of MRF. This process involves fusing intensity gradient, curvature cues, and variance in disparity. The theory of artificial potential field method creates an obstacle avoidance path planning method. Several approaches such as vehicle kinematics, dynamics of obstacle avoidance paths, and the constraints of road boundaries will be

analyzed in this review. Furthermore, there are also complete sections for autonomous vehicle theories and formation control for autonomous vehicles.

2. Technological Perspectives on Autonomous Vehicles

Researchers and scholars have accomplished significant results in the field of autonomous driving over the years. However, many challenges remain to be overcome. The implementation of an autonomous driving environment involves a number of factors such as traffic management strategies and complex technologies [7]. The Society of Automation Engineers (SAE) has recognized six levels of driving automation, which have been adopted by the United States Department of Transportation [1]. These levels range from level 0 to level 5. They rely on on-board driving assistance systems in a connection between the driver and the vehicle. Levels 0 to level 2 are traditional, with the driver controlling the vehicle. Levels 3 to 4 require a vehicle to collect and interpret all necessary data from the surroundings. The vehicle can operate itself in limited special areas, but no human assistant is needed. Level 5 allows the vehicle to perform all driving tasks under any driving conditions autonomously. In 2017, the Volkswagen Group introduced the AUDI A8 to the public as the only model with a SAE3-level. Despite the announcements made by several companies, most predictions indicate that it will be a long time before SAE5-level vehicle technology will be available [7].

A cooperative autonomous driving system relies on several major vectors, such as vehicle structures, reliable communication systems, the cloud, and infrastructure. The design of autonomous driving consists of four distinct parts: the sensing system, the client system, the action system, and the human machine interface (HMI).

The sensing system is for collecting data from surrounding vehicles and the environment. Real-time data must be collected under any type of conditions. A variety of sensors are used to improve the sensing in vehicles, and they support a specific part of the driving assistance. The implementation of the LiDAR sensor, for instance, allows vehicles to have 360-degree vision and the ability to measure distances with a precision of ± 2 cm. LiDAR can also measure distances up to 60m and up to 500m with less precision, and produce accurately 3D maps of nearby objects. Therefore, LiDARs are capable of mapping, navigating, detecting, and tracking obstacles of other vehicles and pedestrians. Self-localizing the vehicles relies on a global navigation satellite system [7].

The client system of an autonomous vehicle consists of the hardware and the operating system required to process the data provided by the sensors. The computing framework must extract in real time accurate and related information from the raw data provided by the sensors, which is called the perception task. In addition, it notifies the vehicle on the progress that must be made, a process known as the decision task. System-on-chip (SoC) solutions are one example of the types of hardware platforms that are being designed for the client systems of autonomous vehicles. They are small integrated circuits with a microprocessor and advanced peripherals. Cloud computing is considered an essential tool to the system, which must support the system if it fails. The perception task consists of three units: localization, detection, and tracking. They work through data fusion and operate at different levels. Localization utilizes algorithms that fuse data from GPS, IMU, and LiDAR, which produces a high-resolution ground map. Vision-based deep-learning technologies, which can autonomously deal with large amounts of data, accomplish accurate results for object detection. Deep-learning techniques support object tracking that is related to approaches based on computer vision. Decision-taking involves prediction, path planning, and obstacle avoidance [7].

The action system comprises the mechanical units of the vehicle, which simulate the steering system, braking system, etc. The mechanical units will improve with other parts of autonomous vehicles. The HMI is minimalist in SAE5-level vehicles. It is set to give information about the driving [7].

Autonomous vehicles require external backup for computing tasks, and a cooperative environment that is supported by communications. Connected Autonomous vehicles (CAVs) must share information about infrastructure, the cloud, pedestrians, and other devices, which is known as V2X communications. Building a powerful, reliable, and safe communications network is still under study. The network must allow large amounts of data to transmit at high speed with minimum latency under conditions, such as climate conditions, traffic state, etc. Also, it must be protected from threats, such as failure conditions, hackers, and terrorist attacks. The penetration ratio of AVs must be high. In addition, the cooperative traffic management strategies must operate sufficiently. These situations are important and must be satisfied to accomplish successful results. In addition, the compatibility of different countries must be ensured. Globally, two tendencies are followed: the implementation of evolutions of wireless standard 802.11p or of mobile networks 5G [8,9,10].

The cloud under a strong communications network supports vehicles in data storage and calculation, for example, by uploading maps with high definition and distributed processing. Vehicular ad hoc networks (VANET) will be improved by the communications network, which is created by vehicles in the same environment and perform as nodes on the basis of V2I, V2V, communications [11]. As a result of vehicle movement, VANETs become unsteady and cover only short ranges. Also, they are designed to support tasks that are associated with safety, navigation, and automated toll payment. VANET could be integrated into the cloud to perform varieties of significant tasks. The integration is known as Vehicular Cloud Network (VCN) [12,13].

In order to help AVs preform the perception tasks, the infrastructure needs to be technologically developed. For instance, the shapes and the appearances of the road signs must be clear, the road structures must be smooth, and the implementation of V2I-related technologies must be presented [14,15].

2.1. The Impact of Autonomous Vehicles on Mobility and Traffic Efficiency

The initial designs for AVs were created to ensure safety and convenience. For instance, the time gap taken in AV driving is longer than it is in human driving [16]. Driving behaviors, such as acceleration, deceleration, and lane changing should be under some specific scenarios and have smooth transitions. However, many studies indicated that traffic congestion would grow if a high number of AVs were presented in the traffic stream with these driving behaviors. Around 600 vehicles, hour, lane for an average highway is the loss in capacity that has been evaluated [7,17]. The solution relies on the connection between vehicles, sharing information, and making cooperative decisions related to safety and the global efficiency of the system. The concept of driving automation depends on the application of dynamic traffic management strategies that support important and coordinated technologies. The strategies must be created to handle a variety of traffic condition and slowly get adjusted to the increment in the AVs' rates.

Highway traffic is the most controlled traffic environment that is suitable for examine the required available technology. One of the first traffic management strategies to be implemented is highway platooning. Highway platooning systematizes AVs' movements. Therefore, the distances between vehicles will be minimized at high speed, which makes traveling safer. The platooning strategy

has been implemented by several freight truck companies under certain conditions. The implantation utilized SAE2-level vehicles that have additional ad-hoc platooning equipment. However, there are many challenges with respect to generalized highway platooning: the lowest required level for vehicle automation, kind of vehicles, platoon average space, average speed, and maximum length, shared and dedicated lanes or roads with respect to their exchange with traditional vehicles. Another main challenge is the method that allows vehicles to engage or depart the platoon [7]. For example, a study of “Formation Control for a Fleet of Autonomous Ground Vehicles” by the University of Essex (UK) focused on new stages in autonomous vehicle cooperation, which involves vehicle platooning or formation control. The new steps cover approaches that simulate formation controller design, descriptions and analyzing the methods that identified the approaches. These contributions are specialized for autonomous driving platoons. This technology will improve platooning and advance traffic management strategies. In addition, while developing the efficiency of the presence of AVs, the safety of human drivers must be secured [18].

Vehicle formation control is a platoon-based formation that allows vehicles on the road to follow each other. It is an essential part of traffic management as it has several advantages, such as fuel efficiency, enhanced safety, and decreased road congestion. The implementation of a platoon-based formation for vehicles controlled by humans is straightforward and can be performed daily. However, connected autonomous vehicles (CAV) must remain in the lanes and follow nearby vehicles by keeping a safe distance and velocity. The objective of the platoon formation control is to ensure that the movements of all vehicles in a platoon have the same speed while keeping a required formation geometry, which is determined by a desired inter-vehicle spacing strategy [19]. Hence, certain algorithms, controllers, and strategies for containing longitudinal and lateral control are required for autonomous vehicles to structure a platoon formation. In addition, communication and sharing information between vehicles are an essential part of a formation control and overall operation (ie, collaboration within vehicles). The collaboration relies on a vehicular network that is capable of sensing and information sharing. Making those operations autonomous to reach the desired level of control is a challenge. Therefore, collaboration between vehicles in a dynamic environment needs to be studied. Fig. 1 depicts recent approaches to formation control [18].

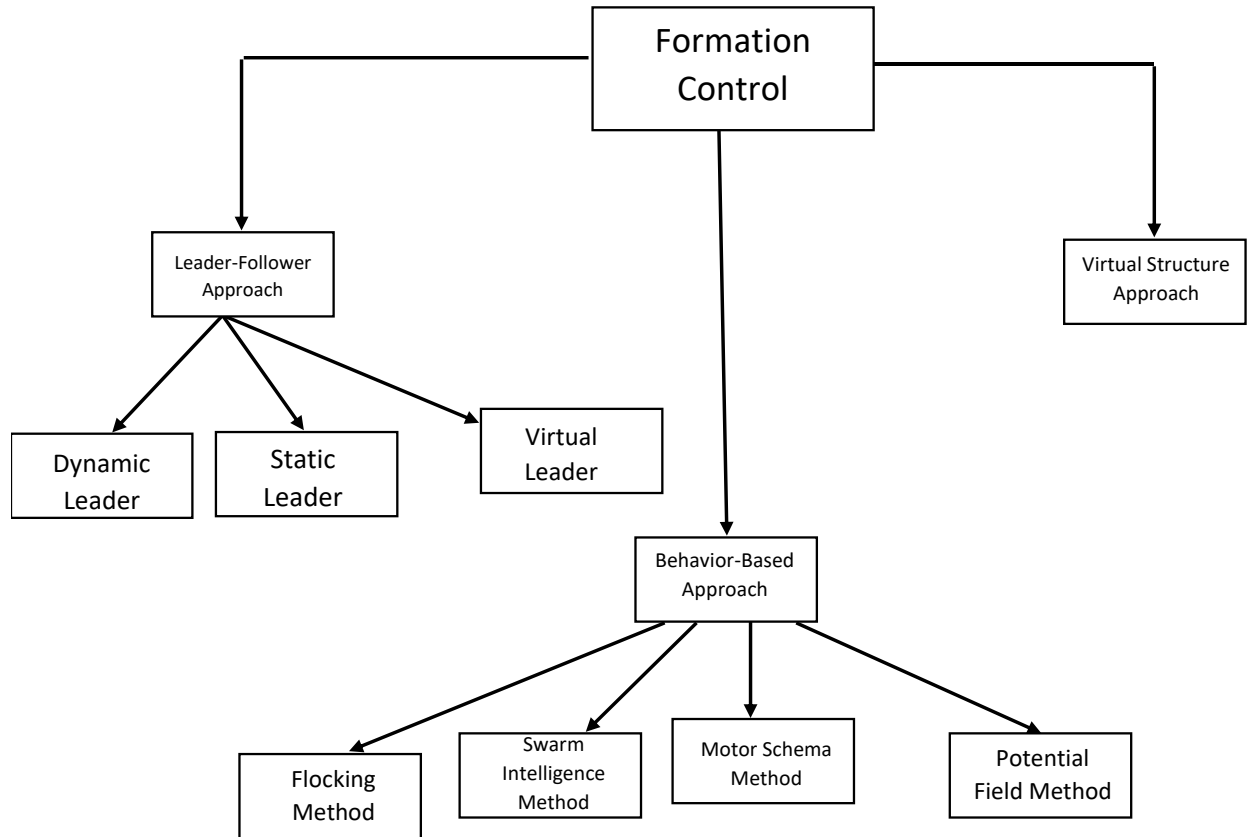


Fig. 1: Formation control approaches [18]

A leader is set to the multi-robot formation in the leader-following approach and the rest of the robots are the followers. The approach allows a leader to follow its required trajectory while robots track the location of the leader. This approach contains three types of leaders: dynamic leader, static leader, and virtual leader. The leader–follower approach benefits include decreased tracking errors, and that the approach can be studied by applying standard control techniques [20]. In addition, trajectories are planned by the leader, while the followers must pursue the coordinates of the leader. Hence, the approach results in a simple controller. The disadvantages of the approach include that a leader’s error may shut down the entire formation and block feedback from followers to a leader [18].

The behavior-based approach is a structured network of interacting behaviors, in which the last action of every robot is derived by the behavior coordinator. In this approach, every single robot presents several behaviors related to sensory inputs, which simulate obstacle avoidance, goal seeking, and formation keeping so that final control is obtained from the weighting of the importance of each behavior. This approach contains four major methods: flocking, swarm intelligence, motor scheme, and potential field. The behaviors coordinator sums and normalizes the outcomes of the multiplications of output of every behavior and its relative weight. The advantages of the behavior-based approach include that it can work in an unidentified and dynamic environment due to it being a parallel, real-time and distributed method, and demanding lower formation sharing [18]. Also, every behavior has its physical meaning and the formation feedback

can be combined with group dynamics by matching the outcomes of every single behavior. The requirement for deriving a mathematical model of group dynamics, examining the convergence of particular formations, and securing the stability of the entire formation are some of the approach disadvantages [21].

In the virtual structure approach a virtual rigid structure is derived, which introduces a form of agents. Next, the required virtual rigid structure motion is given, and the motion of the agent is derived from the given rigid structure. In order to track the agents, every single controller has a tracking agent that is derived where the formation is kept by reducing the error between the virtual structure and the current agent position. The desired trajectory in this approach does not support a single agent. However, the entire formation team shared it. The benefit of using this approach is that the coordinated behavior for the entire group is simple to prescribe [20]. The disadvantages of this approach include that because it is centralized, a single error could shut down the whole system. In addition, the performance of the system could degrade due to communication density and calculating burden that are focused on the centralized positions [22].

2.2. Obstacle Detection and Navigation Safety for Autonomous Vehicles

The controller in an autonomous vehicle visual navigation system captures images and possesses information, which allows the vehicle to navigate safely. Researchers have proposed three alternative models that discuss the improvement of a safe autonomous driving system to be implemented in unexpected and hazardous environments: the first model implements various stochastic techniques which use gradient potential, curvature prepotential, and depth variance potential to segment obstacles in the image from the frames of Markov random field (MRF). The techniques calculate the pixel-level images, which allows them to produce valuable information that can be saved in the orientation. In the method, every significant pixel in the node was distributed in MRF. In addition, the AND gate was used in this method to incorporate the outcomes of previous techniques. The second model utilizes semantic segmentation technology to segment path, filter outliers, and other major obstacles. The third model is applied to estimate the angle of the autonomous vehicle's steering wheel. The determination of the threat factor (T_{tf}) is based on studying unexpected obstacles on the roads. The threat factor supports the model identifying the importance of the obstacle, which indicates whether the obstacle is a threat or not [23]. The input of the system composed of optical encoders that were applied for applications used angle detection, such as steering angle sensor (SAS) in vehicles and two stereo images. The applications were also used to compute depth by implementing a semi-global block matching algorithm (SGBM) [24]. The computation of the three cues – disparity variance, depth curvature, and image gradient – is based on depth variance and color images. These cues were incorporated into a unary potential in an MRF and a pairwise potential. Next, the implementation of the standard graph cuts was utilized to get the obstacle. Furthermore, deep learning-based semantic segmentation was applied for road segmentations and extracting the abnormal values. Fig. 2 demonstrates the structure of detection of hazard object and prediction of steering wheel angles [23].

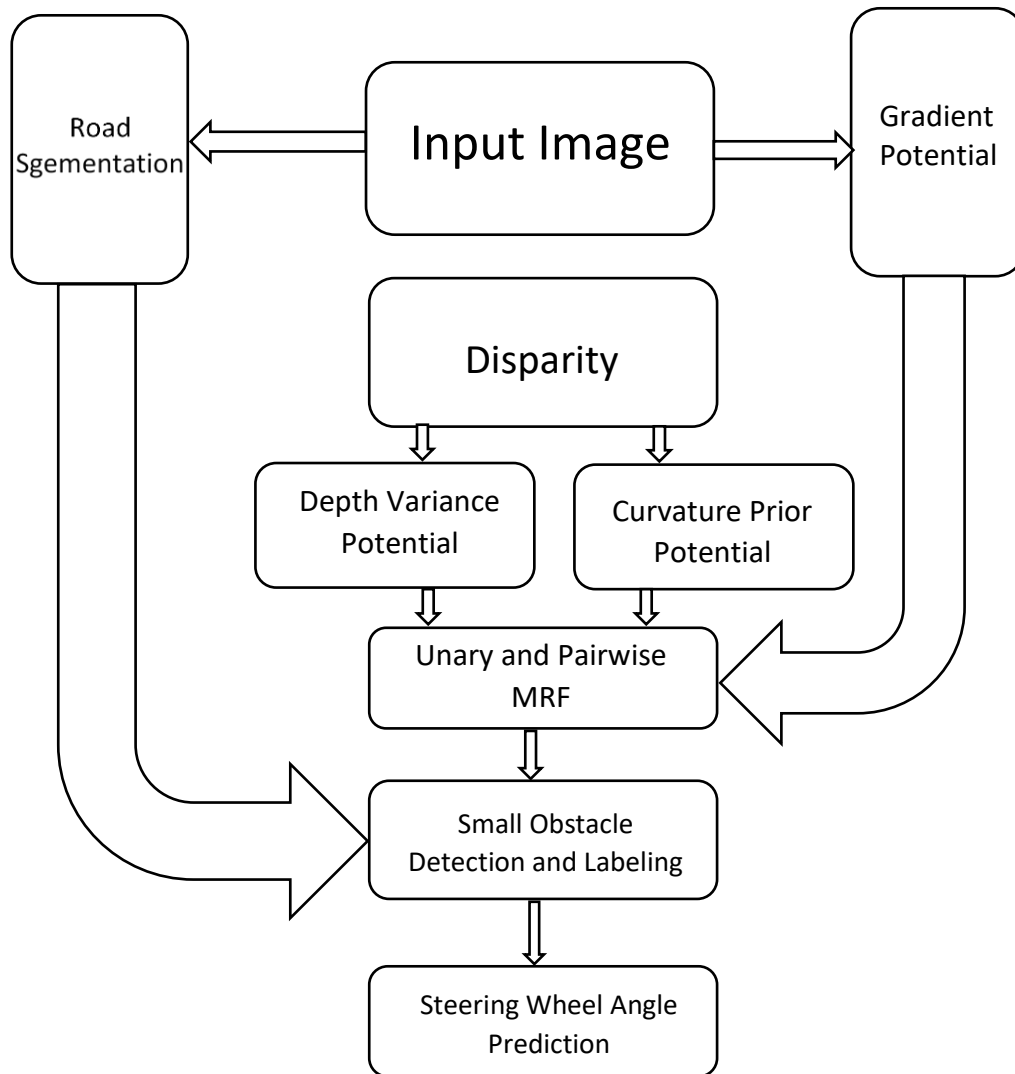


Fig. 2: Structure of detection of hazard object and prediction of steering wheel angles [23]

2.2.1. The Markov Random Field (MRF) Model

Over the years, many studies have been conducted on different MRF models, learning methods, and inference. The studies contribute to improving methods that can fix many low-level, medium-level, and high-level vision issues [25]. The focus in this part of the research was on-the-road small obstacle segmentation, which defines an energy function over an MRF. To solve problems such as image restoration, reconstruction, segmentation, edge detection, 3D vision, and object labeling in the image, inference concerns underlying the image and scene structure must be addressed [26]. The image, element X_s , and random process X were combined, in which $s \in S$ is a position of a pixel in the image. The position of every pixel in the image is evaluated as a node in the MRF and associated with every node with the unary or pairwise cost [27]. The following equation describes minimum energy function E :

$$E(X) = \sum_s E_u(s) + \sum_{(r,s) \in N} E_p(X_r, X_s) \quad (1)$$

Where $E_u(s)$ is the unary term, $E_p(X_r, X_s)$ is the pairwise term, and X is a set of random variables that is associated with the set of nodes S . The set of nodes S gets label $x_s \in [0,1]$, which relies on the kind of natural appearance, whether it is a road, a small obstacle on a road, or texture. Around every pixel, the computation of the unary $E_u(s)$ was made separately. The unary $E_u(s)$ term consists of a combination of three cues: gradient potential $E_u^g(s)$, depth curvature potential $E_u^c(s)$, and depth variance potential $E_u^v(s)$. The following equation demonstrates the unary $E_u(s)$ term [23]:

$$E_u(s) = E_u^g(s) * E_u^c(s) * E_u^v(s) \quad (2)$$

2.2.2. Gradient Potential

The following equation represents the potential gradient at the site (i, j) :

$$E_u^g(i, j) = \sqrt{G_x(i, j)^2 + G_y(i, j)^2} \quad (3)$$

In the original color image, the calculations of partial derivative $G_x(i, j)$ and $G_y(i, j)$ are in the vertical and horizontal lines [23,28].

2.2.3. Curvature Prior Potential

Curvature is the reciprocal of the radius of a circle that is tangent to the presented curve at a point. “0” represents a straight-line curvature and curvature “1” symbolizes a curve. Curvature usually happens when the small circles are bent sharply. Therefore, the autonomous vehicles utilize this feature in several functions, such as free space detection and curb detection [29,30]. The algorithm determines the changes along the normal surface when operating an Eigen analysis close to the 3D point. The following equation illustrates the curvature potential:

$$E_u^c(s) = \frac{\sqrt[2]{\lambda_3}}{\sqrt[2]{\lambda_1} + \sqrt[2]{\lambda_2} + \sqrt[2]{\lambda_3}} \quad (4)$$

Where $E_u^c(s)$ represents the curvature prior at the corresponding position gained after the 3D point in the image space. The $\sqrt[2]{\lambda_3}$ of eigenvalue $(\lambda_1, \lambda_2, \lambda_3)$ can identify as nonplanar surfaces. The characteristic of curvature prior does not produce a plane surface assumption extremely clearly, which makes it robust and more stable [23].

2.2.4. Depth Variance Potential

The potential for detecting sudden changes in depth can be computed when the slide horizontally on the image is used [31]. The calculation procedures are based on summation of the sudden depth horizontal windows (W_h) in square window (W_s) , in addition to multiplying the outcome by

corresponding disparity can be seen in the pixel even in cases that the obstacles do not appear. The depth variance equation is presented as [23]:

$$D_{var}(i, j) = var \left(\left[D \left(i - \frac{W_h}{2}, j \right) : D \left(i + \frac{W_h}{2}, j \right) \right] \right) \quad (5)$$

Therefore, D is the depth map.

The final variance potential is introduced as:

$$E_u^v(i, j) = \left(\sum_{a=-\frac{W_s}{2}}^{\frac{W_s}{2}} \sum_{b=0}^{W_s} D_{var}(i + a, j - b) \right) * d(i, j) \quad (6)$$

Therefore, $d(i, j)$ is the parallax value of the specific located pixel (i, j) .

2.2.5. Pairwise Potential

The pairwise potential was determined by implementing the Potts model [23]:

$$E_p(X_r, X_s) = -J_p \sum_{(r,s)} \delta(X_r, X_s) \quad (7)$$

Hence, $\delta(X_r, X_s)$ is Kronecker delta. The value is 1 when $X_r = X_s$; otherwise it is 0. The global minima of energy function of road-detected small obstacle is presented by the following equation:

$$X^* = \underset{x}{argmin} E(X) \quad (8)$$

The graph cut feature supports the global minima efficiently.

2.2.6. Identifying the Obstacle Threat Value in the Image

The threat value is defined by detecting obstacles in the capture image. Semantic segmentation and MRK mode help determine the obstacle coordinate (x, y) in the capture image. The calculation of the threat value can be achieved by measuring the distance of the obstacles from the bottom center of the pixel $(h, \frac{w}{2})$ in the image height (h) and width (w) . The following formula defines the threat value:

$$T_{tf} = 1 - \sqrt{\frac{(x-h)^2 + (y - \frac{w}{2})^2}{h^2 + (\frac{w}{2})^2}} \quad (9)$$

Therefore, T_{tf} represents the threat value, h is the image height, and w is the image width. Deducting the value of the height with half of the width from the values of the x and y ,

respectively, yields the latitudinal and longitudinal distance from the center line of the obstacle [23].

3. Design of Obstacle Avoidance Path Planning for Autonomous Vehicles Using an Improved Artificial Potential Field Algorithm

3.1. Analysis of obstacle avoidance process and maneuver

Vehicle collision risk assessment and obstacle avoidance path planning are the two units of obstacle avoidance maneuvers for autonomous vehicles. Obstacle avoidance processes operated by humans rely on the perception of dynamic traffic scenarios, thus completing path planning and obstacle avoidance decision-making. Obstacle avoidance behavior consists of five sub-behaviors as shown in Fig. 3 [32].

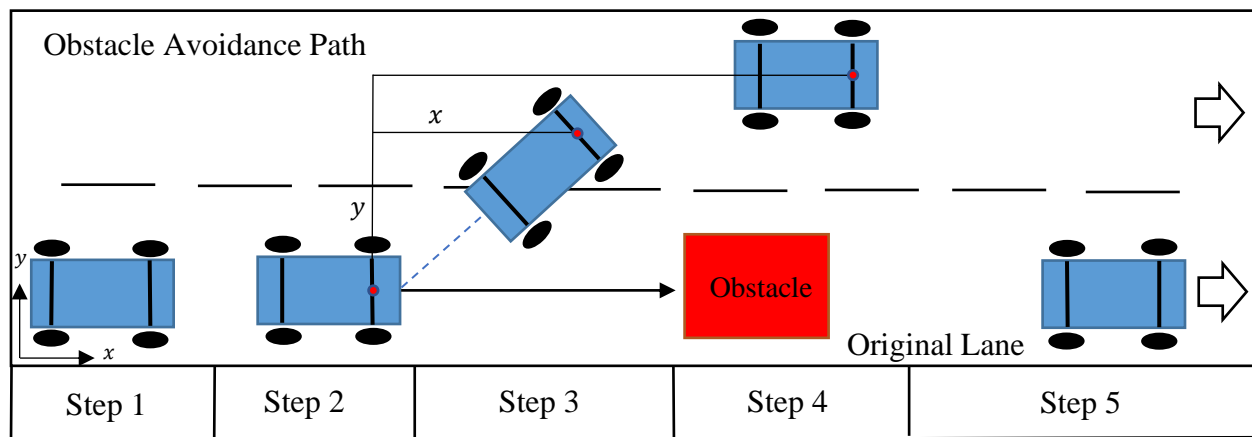


Fig. 3: The processes of obstacle avoidance [32]

Step 1: Detection for obstacle avoidance: Determine if a vehicle's current situation matches the criteria of obstacle avoidance, such as obstacles on the road, the speed of ego vehicle is higher than the obstacle, and adequate space to avoid an obstacle.

Step 2: Path planning and calculation: Environmental information enables a collision-free path.

Step 3: Changing lane to avoid obstacle: A lane-changing maneuver is executed to track the created obstacle avoidance path.

Step 4: Passing: After the lane change, the obstacle is avoided.

Step 5: Return to original lane: Ego vehicle returns to the original lane after the obstacle is avoided over a specific distance.

3.2. Obstacle-Avoidance Safety Model

Approximately 30% of traffic accidents occur during lane-changing, according to the National Highway Traffic Safety Administration (NHTSA) [33]. Researchers have suggested a lane change hazard perception model that relies on the behavior of human drivers to decrease the number of deaths and injuries [34]. Results indicate that the danger of traffic accidents depends on the speed, movement state, and properties of obstacles [35]. To ensure safety, drivers need 0.3-1s to predict risk advance [36]. The simplified obstacle-avoidance model relies on the driver-risk model and

driver-behavior characteristics. An examination of the performance characteristics of human drivers makes it clear that the parameter of obstacles has an impact on Step 1. For instance, if the obstacles in front of the driver are large, human drivers have the time to implement obstacle-avoidance maneuvers. To avoid a larger volume obstacle or trend of lateral movement in Steps 3 and 4, drivers increase steering angle and retain more lateral distance to avoid an obstacle. Non-stationary obstacles, such as pedestrians, traffic participants, and obstacle vehicles are complex and challenging to handle during the actual driving. In addition, strategies for obstacle avoidance that target moving and stationary obstacles are different in real-time scenarios. Based on the study of autonomous driving vehicles, the computation results of Step 2 would have an immediate impact on the follow-up operation of obstacle avoidance, which relies on the control precision of actuators. The collision probability in Step 3 is higher than in the other steps. A collision not occurring in Step 3 indicates that the ego vehicle bypasses the obstacle successfully. Hence, the creation of the obstacle-avoidance safety model is required to ensure the safety of the obstacle-avoidance path. As depicted in Fig. 4, the following equation illustrates the condition for collision avoidance between vehicle and obstacle.

$$X_{ego} + w \sin \theta < X_{obs} + S \quad (10)$$

Where X_{ego} is the ego vehicle longitudinal displacement during the time of performing obstacle avoidance, X_{obs} is the longitudinal displacement of the obstacle vehicle during the time of ego vehicle performing obstacle avoidance. S is the starting distance between the ego vehicle and the obstacle vehicle, W is the ego vehicle width, and θ is the angle between the lane and the x-axis of the vehicle coordinate. The lateral velocity is related to the value of the angle [32].

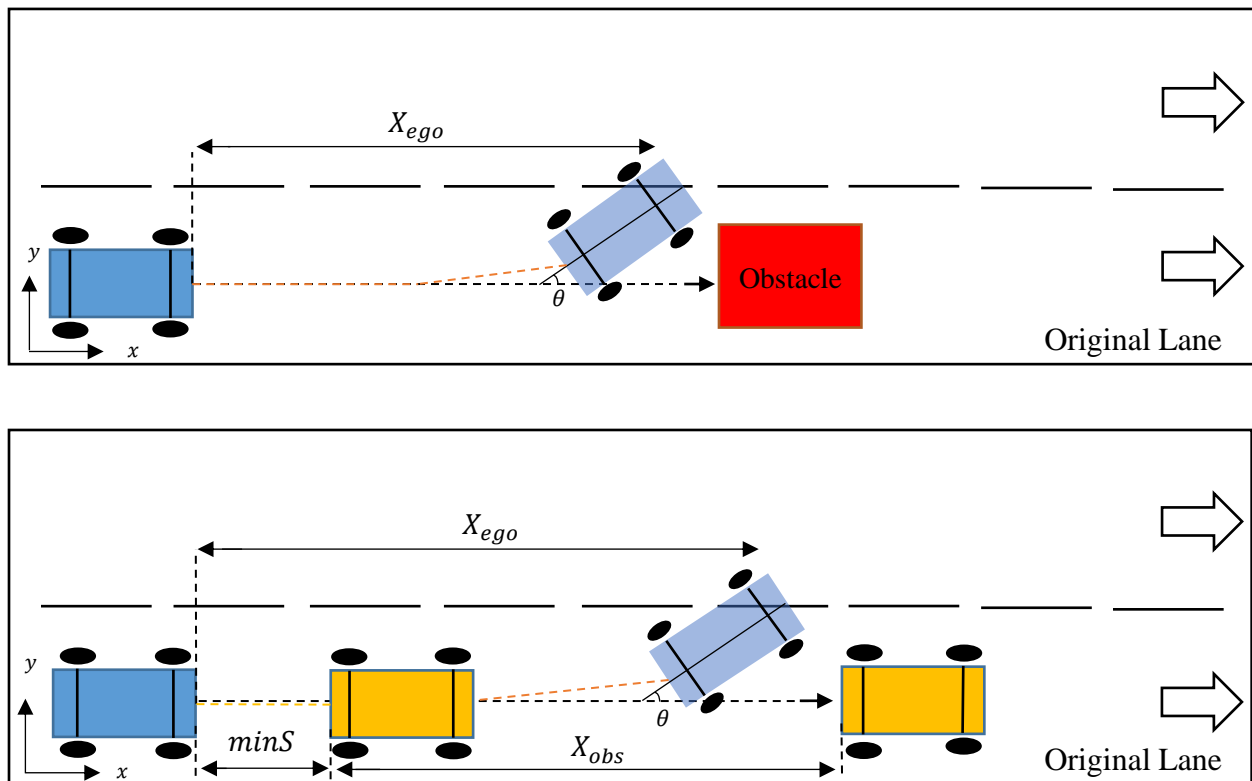


Fig. 4: Longitudinal safety distance between obstacle and ego vehicle [32]

The ego vehicle longitudinal displacement during the interval of obstacle avoidance operation is presented as the following:

$$X_{ego} = \int_0^{t_c} \dot{X}_{ego} dt \quad (11)$$

The obstacle vehicle longitudinal displacement during the interval of the ego vehicle obstacle avoidance operation is presented as the following:

$$X_{obs} = \int_0^{t_c} \dot{X}_{obs} dt \quad (12)$$

To ensure that no collision happens during the lane-change process and based on equation (10), the initial distance S can be presented as:

$$S = X_{ego} + w \sin \theta - X_{obs} > 0 \quad (13)$$

Adding the above equations to the kinematic relationship of vehicles in the obstacle-avoidance process, the minimum longitudinal safety distance that is needed to finalize obstacle avoidance without collision is:

$$\min S = \{(\dot{X}_{ego} - \dot{X}_{obs})t_c + \int_0^{t_c} (\ddot{X}_{ego}(t) - \ddot{X}_{obs}(t))dt + w \sin \theta, 0\} \quad (14)$$

The relative velocity of overtaking is low in real-life traffic scenarios. Hence, larger errors occur in the computation outcomes of equation (14), which was developed to ensure driving safety. The development involves time headway and driver behavior characteristics:

$$\min D = \min S + c(\dot{X}_{obs} - \dot{X}_{ego}) + d_0 + \sigma(\dot{X}_{obs} - \dot{X}_{ego}) \quad (15)$$

Where c is headway, d_0 represents safety breaking distance, and σ denotes the obstacle risk factor, which introduced as:

$$\sigma = \frac{G_1 * m_{obs} * w_{obs}}{G_2 S} \exp G_3 \max\{(\dot{X}_{ego} - \dot{X}_{obs}), 0\} \quad (16)$$

Where m_{obs} is the mass of obstacle, and w_{obs} is the width of obstacle. Adjustment coefficients are G_1 , G_2 , and G_3 . Human driver obstacle avoidance and obstacle-avoidance path planning based on artificial potential field share the same principles. The main concept is to provide a collision-free path and adjust an appropriate safety margin that depends on the kinds and the movement of obstacles [32].

4. Obstacle Avoidance Path Planning for Autonomous Vehicles

4.1. Artificial Potential Field Design

In 1986, the artificial field potential approach was introduced [37,38]. It focuses on describing realistic senses by building an artificial virtual potential field. The vehicle tracks the path of resultant force that is determined by attraction and reputation, which is produced by the obstacle and the target point. The implementation of classical artificial potential field algorithm cannot be used directly on obstacle-avoidance path planning for autonomous vehicles because of its limitations [39]. Hence, the development of proposed artificial potential field approach relies on the improvement of obstacle repulsive field function.

Supposing the position of ego vehicle is:

$$X_{ego}^p = (x_{ego}, y_{ego}) \quad (17)$$

The target position point is:

$$X_{tgt}^p = (x_{tgt}, y_{tgt}) \quad (18)$$

The obstacle position is:

$$X_{obs}^p = (x_{obs}, y_{obs}) \quad (19)$$

The target point produces gravity in the artificial potential field. The target point gravitational field is:

$$U_{att} = \frac{1}{2} k_{att} (X_{ego}^p - X_{tgt}^p)^2 \quad (20)$$

Where k_{att} represents the coefficient of the gravitational potential field.

The ego vehicle pursues the target point under the effect of the gravity that is created by the target point. The value of gravitation reduces with the distance. Hence, the ego vehicle gravitational force represents the negative gradient equation of the target point potential field:

$$F_{att} = -\nabla(U_{att}) = k_{att} a_{att} \quad (21)$$

According to the artificial potential field, obstacles create repulsive fields. The following equation illustrates the gravitational field of an obstacle:

$$U_{rep} = \begin{cases} \frac{1}{2} k_{rep} \left(\frac{1}{\rho_0} - \frac{1}{\rho_{obs}} \right)^2, & \rho_{obs} > \rho_0 \\ 0, & \rho_{obs} \leq \rho_0 \end{cases} \quad (22)$$

Where k_{rep} represents the coefficient of the repulsive potential field, ρ_{obs} is the obstacle-repulsive potential field radius, ρ_0 denotes the distance between the obstacle and the ego vehicle, the following equation demonstrates the repulsive force on the ego vehicle:

$$F_{rep} = \begin{cases} k_{rep} \left(\frac{1}{\rho_0} - \frac{1}{\rho_{obs}} \right) \left(\frac{1}{\rho_0} \right)^2 a_{rep}, & \rho_{obs} > \rho_0 \\ 0, & \rho_{obs} \leq \rho_0 \end{cases} \quad (23)$$

In normal driving conditions, the longitudinal velocity is larger than lateral velocity. The obstacle-avoidance path quality and smoothness should be evaluated. Consequently, the potential field of obstacles is developed to ellipse.

$$\frac{x_{obs}^2}{A^2} + \frac{y_{obs}^2}{B^2} = 1 \quad (24)$$

The combination of safety constructed optimized the parameters of the obstacle's potential field.

$$A = \min D \quad (25)$$

$$B = \delta \sigma * \frac{w_{obs}}{2} \quad (26)$$

Where δ denotes the adjustment coefficient of the repulsive field that is applied to adjust the range of the potential field and w_{obs} represents the width of an obstacle. The following equation shows the repulsive force:

$$F_{rep} = \begin{cases} k_{rep} \left(\frac{1}{\rho_0} - \frac{1}{\rho_{obs}} \right) \left(\frac{1}{\rho_0} \right)^2 a_{rep}, X_{ego}^p \in \frac{x_{obs}^2}{A^2} + \frac{y_{obs}^2}{B^2} = 1 \\ 0, X_{ego}^p \notin \frac{x_{obs}^2}{A^2} + \frac{y_{obs}^2}{B^2} = 1 \end{cases} \quad (27)$$

When the obstacle, the ego vehicle, and the target point are in a line, repulsion is created by the obstacle and gravitation created by the target point acting on the ego vehicle in the process of obstacle avoidance. Consequently, the ego vehicle resultant force acting would be zero, and stopping of the ego vehicle might occur, reaching to a local minimum where the target point could be unreachable. A virtual target point is implemented to solve this issue. Two virtual target points were used: the first virtual target point is stationed in the target lane. The second virtual target point is in the external range of the obstacle potential field in the original lane. The gravitation created by the virtual target point could guide the ego vehicle, leaving the local minimum point [40].

4.2. Constraint Analysis for Avoidance the Obstacles

The motion of a vehicle should fulfill the constraints of dynamics, vehicle kinematics, and roads. Based on road structures, the middle lane is the safest to drive when there are no obstacles. Recurrent lane-changing should not occur unless it is mandatory. To avoid unnecessary lane-crossing, lane boundaries are proposed. Artificial potential fields are described for lane lines:

$$U_{road} = \begin{cases} k_{road} \exp \left(\frac{w_{lane}}{2} - l_{ego}^l \right), l_{ego}^l \in \left(\frac{w_{ego}}{2}, \frac{w_{lane}}{2} \right) \\ 0, l_{ego}^l, l_{ego}^r \notin \left(\frac{w_{ego}}{2}, \frac{w_{lane}}{2} \right) \\ k_{road} \exp \left(\frac{w_{lane}}{2} - l_{ego}^r \right), l_{ego}^r \in \left(\frac{w_{ego}}{2}, \frac{w_{lane}}{2} \right) \end{cases} \quad (28)$$

Where, k_{road} denotes the coefficient of the potential field, l_{ego}^r represents the distance between the right lane line and the ego vehicle, w_{lane} is the lane width, and w_{ego} is the vehicle, based on the proposed lane boundaries, the vehicle can remain in the center of the lane even after moving to the next lane [32].

The boundaries of the road and obstacles, the path created by improved artificial potential field function that adopts the dynamic constraints of the vehicle, should be evaluated. The lane-changing maneuver for the ego vehicle happens twice during the obstacle-avoidance process. The dynamic steering stability of the vehicle will be impacted by an angle that is significantly large. Hence, the stability of the steering angle and speed should be under specific conditions in order to ensure the performance and stability of the steering in addition to the driving safety. The threshold $\frac{4}{10}g$ should not be surpassed by tire stiffness and the lateral acceleration of the vehicle [41]. The lateral acceleration of the vehicle should not surpass $\frac{75}{100}\mu g$ to avoid sideslipping [42,43]. To achieve the stability of obstacle avoidance, vehicle lateral acceleration constraint could be shown:

$$\min a_y = \min\{0.4g, 0.75\mu g\} \quad (29)$$

According to the two-degree-of-freedom vehicle model [40], the equation between lateral acceleration and front wheel angle is given:

$$|\beta_{lim}| = \left| \frac{\min a_y (1 + K v_x^2) l}{v_x^2} \right| \quad (30)$$

Where K denotes the stability factor of the vehicle, β denotes the angle of the front wheel, l is the vehicle wheelbase, and v_x represents the longitudinal velocity of vehicle. To ensure the vehicle steering stability and based on the study above, the value of the front wheel angle should fulfill [32]:

$$|\beta_{real}| < |\beta_{lim}| \quad (31)$$

5. Conclusion

This paper summarizes many academic published papers that show the most recent developments in autonomous vehicle technology. The developments include AV theories, formation control, obstacle detection, and obstacle-avoidance strategies. The AV theories present a concept of the integration of autonomous vehicles on the road and future challenges. Formation control gives an example for the approaches that simulate vehicle formation control. Obstacle detection and avoidance strategies introduce the steps which allow an autonomous vehicle to navigate safely. A Markov random field (MRF) was applied for obstacle detection. The applications provide a unique background to analyze the improved algorithms. Hence, it can be summarized that obstacle-avoidance strategies include an obstacle-avoidance path-planning approach that relies on the performance of an obstacle-avoidance system. Analyzing the obstacle-avoidance behavior of a human driver contributes to create a safety model of the obstacle-avoidance system. Improvement of the artificial field method is based on the safety model. In addition, the repulsive field range of obstacles is generated. Building autonomous driving vehicles' collision-free path depends on improving the artificial potential field. Future work could cover a variety of obstacles, variable speeds, and decision-making for the obstacle avoidance path planning in complex environments.

References

- [1] “What is an Autonomous Car?,” Synopsys, Inc. [Online] Available: <https://www.synopsys.com/automotive/what-is-autonomous-car.html>
- [2] “What is an autonomous vehicle? Definition and meaning,” Market Business News. [Online] Available: <https://marketbusinessnews.com/financial-glossary/autonomous-vehicle/>.
- [3] “Road traffic injuries,” World Health Organization. February 7, 2020. [Online] Available: <https://www.who.int/news-room/fact-sheets/detail/road-traffic-injuries>
- [4] “Traffic Safety Facts,” NHTSA. May 2019. [Online] Available: <https://crashstats.nhtsa.dot.gov/Api/Public/ViewPublication/812753>
- [5] “MANAGING A SLOW REACTION TIME,” DriveSafety. [Online] December 3, 2018. Available: <https://drivesafety.com/managing-a-slow-reaction-time/>
- [6] A. Jarvis, “An Introduction to Autonomous Cars: How They Will Improve the Cost, Convenience, and Safety of Driving,” Velodyne Lidar Inc. September 19, 2018. [Online] Available: https://velodynelidar.com/blog/an-introduction-to-autonomous-cars-how-they-will-improve-the-cost-convenience-and-safety-of-driving/?utm_source=rss&utm_medium=rss&utm_campaign=an-introduction-to-autonomous-cars-how-they-will-improve-the-cost-convenience-and-safety-of-driving.
- [7] M. Martínez-Díaz, F. Soriguera, (2018). Autonomous vehicles: theoretical and practical challenges. XIII Conference on Transport Engineering, CIT2018. Available: www.sciencedirect.com
- [8] Intel GO™ Automated Driving Solutions Automated driving, accelerated., Intel, 2016.
- [9] J. Arriola, “Automated and connected driving,” Report of Federal Minister of Transport and Digital Infrastructure. Rep 216, 18-27, 2017.
- [10] S. Shaheen, H. Totte. A. Stocker. “Future of Mobility White Paper,” UC Berkeley, UCCnect. 2018.
- [11] S. Zeadally, et al. “Vehicular ad hoc networks (VANETs): status, results, and challenges,” Telecommunication Systems 50, 2012, pp. 217-241.
- [12] E. K. Lee, et al. “Internet of vehicles: From intelligent grid to autonomous cars and vehicular clouds,” IEEE World Forum on Internet of Things (WF-IoT), Seoul, South Korea, 2014.
- [13] F. Ahmad, M. Kazim, A. Adnane, A. Awad,” Vehicular Cloud Networks: Architecture, Applications and Security Issues,” IEEE/ACM 8th International Conference on Utility and Cloud Computing (UCC), Limassol, Cyprus, 2015.
- [14] P. Bosetti, M. Da Lio, A. Saroldi, “On Curve Negotiation: From Driver Support to Automation,” IEEE Transactions on ITS 16, 2015, pp. 2082-2093.
- [15] A. García, F. J. Camacho, P. V. Padovani, “Influence of road infrastructure on the speed of automated vehicles,” ISSN 0212-6389, N° 216, 2017, pp. 52-61.
- [16] C. Diakaki, et al. “Overview and Analysis of Vehicle Automation and Communication Systems from a motorway traffic management perspective,” Transportation Research Part A: Policy and Practice 75, 2015, pp. 147–165.
- [17] A. I. Ntousakis, K. I. Nikolos, M. Papageorgiou, “On Microscopic Modelling of Adaptive Cruise Control Systems,” Transportation Research Procedia 6, 2015, pp. 111–127.
- [18] A. Soni, H. Hu, “Formation Control for a Fleet of Autonomous Ground Vehicles: A Survey,” Journal of Robotics, 2018, doi:10.3390.
- [19] P. Kavathekar, Y.Q. Chen, “Vehicle Platooning: A Brief Survey and Categorization,” IEEE International Conference on Mechatronic and Embedded Systems and Applications, Washington, DC, USA, August 2011, pp. 28–31.

- [20] J. Chunyu, Z. Qu, E. Pollak, M. Falash, “A New Multi-objective Control Design for Autonomous Vehicles,” *Optimization and Cooperative Control Strategies*, Hirsch, M.J., Commander, C.W., Pardalos, P.M., Murphey, R., Eds.; Springer: Berlin/Heidelberg, Germany, 2009; pp. 81–102; ISBN 978-3-540-88063-9.
- [21] J.R.T. Lawton, A.W. Beard, J. B. Young, “A Decentralized Approach to Formation Maneuvers.” *IEEE Trans. Robot. Autom.* 2003, 19, pp. 933–941.
- [22] W. Ren, W. R. Beard, “Decentralized Scheme for Spacecraft Formation Flying via the Virtual Structure Approach,” *J. Guid. Control Dyn.* 2004, 27, pp.73–82.
- [23] M. Haris, J. Hou, “Obstacle Detection and Safely Navigate the Autonomous Vehicle from Unexpected Obstacles on the Driving Lane,” *Sensors* 2020, 20, 4719; doi:10.3390/s20174719.
- [24] H. Hirschmuller, “Stereo Processing by Semiglobal Matching and Mutual Information,” *IEEE Trans. Pattern Anal. Mach. Intell.* 2007, 30, pp. 328–341.
- [25] C. Wang, N. Komodakis, N. Paragios, “Markov Random Field modeling, inference & learning in computer vision & image understanding: A survey,” *Comput. Vis. Image Underst.* 2013, 117, pp. 1610–1627.
- [26] S.Z. Li, “Markov Random Field Modeling in Image Analysis,” Springer Science and Business Media, New York, NY, USA, 2001.
- [27] B. Savchynskyy, “Discrete Graphical Models—An Optimization Perspective,” *Found. Trends Comput. Graph. Vis.* 2019, 11, pp.160–429.
- [28] A. Freno, E. Trentin, “Markov Random Fields,” Springer: Berlin, Heidelberg, Germany, 2011.
- [29] M. Pauly, M. Gross, L.P. Kobbelt, “Efficient Simplification of Point-Sampled Surfaces,” *Proceedings of the IEEE VIS*, Boston, MA, USA, 27 October–1 November 2002, pp. 163–170.
- [30] C. Fernandez, D. Fernández-Llorca, C. Stiller, M. A. Sotelo, “Curvature-based curb detection method in urban environments using stereo and laser,” *Proceedings of the IEEE Intelligent Vehicles Symposium (IV)*, Seoul, Korea, 28 June–1 July 2015, IEEE: Piscataway, NJ, USA, 2015; pp. 579–584.
- [31] E. Shabaninia, A. R. Naghsh-Nilchi, S. Kasaei, “High-order Markov random field for single depth image super-resolution,” *IET Comput. Vis.* 2017, 11, pp. 683–690.
- [32] P. Wang, S. Gao, L. Li, B. Sun, S. Cheng, “Obstacle Avoidance Path Planning Design for Autonomous Driving Vehicles Based on an Improved Artificial Potential Field Algorithm,” *Energies* 2019, 12, 2342; doi:10.3390/en12122342.
- [33] R. Paleti, N. Eluru, R. Bhat, “Examining the influence of aggressive driving behavior on driver injury severity in trac crashes,” *Accid. Anal. Prev.* 2010, 42, pp. 1839–1854.
- [34] J. Ji, et al. “Design of 3D Virtual Dangerous Potential Field for Vehicle Active Collision Avoidance,” *Automot. Eng.* 2016, 38, pp. 1065–1071.
- [35] Z. Liu, J. Han, J. Ni, “A Research on Adaptive Lane Change Warning Algorithm Based on Driver Characteristics,” *Automot. Eng.* 2019, 41, pp. 440–446.
- [36] J. Wang, J. Wu, Y. Li, “Concept, Principle and Modeling of Driving Risk Field Based on Driver-vehicle-road Interaction,” *China J. Highw. Transp.* 2016, 29, pp.105–114.
- [37] L. An, et al. “A Simulation on the Path Planning of Intelligent Vehicles Based on Artificial Potential Field Algorithm,” *Automot. Eng.* 2017, 39, pp. 1451–1456.
- [38] N. Wahid, et al. “Study on potential field based motion planning and control for automated vehicle collision avoidance systems,” In *Proceedings of the IEEE International Conference on Mechatronics*, Churchill, VIC, Australia, 13–15 February 2017.

- [39] Y. Rasekhipour, et al. “A Potential Field-Based Model Predictive Path-Planning Controller for Autonomous Road Vehicles,” *IEEE Trans. Intell. Transp. Syst.* 2017, 18, pp. 1255–1267.
- [40] Z. Pan, et al. “Intelligent Vehicle Path Planning Based on Improved Artificial Potential Field Method,” *Appl. Mech. Mater.* 2015, 742, 6.
- [41] Z. Yu, “Automobile Theory,” 5th ed., China Machine Press, Beijing, China, 2009. 30.
- [42] J. Wu, et al. “A Human-Machine-Cooperative-Driving Controller Based on AFS and DYC for Vehicle Dynamic Stability,” *Energies*, 2017, 10, 1737.
- [43] J. Feng, et al. “Research on Methods of Active Steering Control Based on Receding Horizon Control,” *Energies* 2018, 11, 2243.